Materials Science and Technology, 33 (2017)
DOI: 10.1080/02670836.2017.1310431,

Evolution of white-etching cracks and associated microstructural alterations during bearing tests

S. W. Ooi[a], A. Gola[a], R. H. Vegter[b], P. Yan[b], K. Stadler[c]

[a]*Department of Materials Science and Metallurgy, University of Cambridge, 27 Charles Babbage Road, Cambridge. CB3 0FS, U.K.*
[b]*SKF Engineering and Research Centre, Nieuwegein NL 3439 MT, The Netherlands*
[c]*SKF GmbH, Gunnar-Wester-Str. 12, 97421 Schweinfurt,Germany.*

Abstract

The effect of hydrogen and contact pressure on the sequence of microstructural changes during bearing operation has been investigated. The continuation of bearing testing in the presence of microcracks stimulates the formation of (1) white-etching matter (WEM) on the crack surfaces that endure severe surface rubbing, (2) slip bands in the region that experience a higher stress levels due to microcrack formation, and (3) engineering bands within the WEM. Engineering bands are a new observation whereby ferrite crystals cross a multitude of fine grains (WEM). The presence of hydrogen and high contact pressure during the bearing tests promoted early bearing failure, but with the formation of large crack networks, that coexist with slip bands, precursors to WEM, and conventional WEM.

Keywords: White-etching matter, cracks, engineering bands, slip bands

1. Introduction

The white-etching crack (WEC) phenomenon, also called brittle flaking[1,2] and white structure flaking (WSF)[3] as observed in wind turbine and automotive bearings that have failed prematurely, has received considerable attention and is particularly damaging in term of reliability.[3,4,5,6,7] The lack of understanding of its origin makes

Email address: swo23@cam.ac.uk (S. W. Ooi)

predictions or prevention difficult.[8] Only a single branching crack network is needed to stimulate its development into a spall that causes the bearing to fail. In fact, the crack that causes the actual spall becomes damaged during the circumstances leading to gross failure, making it difficult or impossible to trace. The fact that WECs are readily seen in the failed bearings indicates that the number of crack networks developed in the bearing prior to gross failure is large, with the operation of an autocatalytic effect that leads to a rapid escalation of cracking.

There have been several hypotheses regarding the acceleration of crack formation. These include either (i) material weakening by hydrogen[a]; or (ii) load-induced[b]. While the sources of hydrogen entry into the bearing are still being discussed widely,[4] the effect of hydrogen on toughness reduction and acceleration of crack formation in steel is well-known.[7,8,12] There are many reports on the reduction of bearing life due to hydrogen, but not the effect of hydrogen on the sequence of microstructural alteration during rolling contact fatigue.[9] In this work, detailed microstructural studies were performed on bearings that have been tested on known parameters that contain WECs.

2. Experimental procedure

Three investigations have been conducted, two involving type 6309 deep-groove ball bearings (DGBB) and a 7209 angular-contact ball bearing (ACBB). The DGBB inner rings were hydrogen charged using the procedure developed by Vegter.[13] Two different contact stresses were used on the hydrogen charged bearings. The bearing H1 was tested using a contact pressure of 3 GPa whereas H2 was subjected to 2.4 GPa contact stress. A higher contact stress of 3.3 GPa was used on the non-hydrogen charged bearing (S1) in order to initiate failure. The bearing test conditions and predicted bearing life are shown in Table 1. All bearings were made of martensitic ASTM 52100 bearing steel. The measured hardness for all samples is 690±48 HV30.

[a]Source of hydrogen is from the decomposition of lubricating oil, water contamination, aggressive oil additives or stray currents[1,9,6,10]

[b]Via transient loading conditions (for example: impact) or sliding between roller and races),[11,7]

Table 1: The bearing test conditions and parameters used in this work. The predicted bearing life under the testing conditions is also shown.

Parameter	Value	
Bearing type	DGBB	ACBB
Test rig	R2	R2
Contact pressure / GPa	2.4-3.0	3.3
Test temperature/ °C, outer ring	83	60
Speed / rpm	6000	
Lubricant	Shell TT100	Shell TT68
Viscosity ratio/ κ	2.96	4.2
SKF rating life at 90% reliability at 2.4 GPa / Revolutions	2542×10^6	
SKF rating life at 90% reliability at 3.0 GPa / Revolutions	112×10^6	
SKF rating life at 90% reliability at 3.3 GPa / Revolutions	33×10^6	21×10^6

Classic metallographic techniques have been used to characterise the failed sample. The metallographic investigation was performed on the parallel section of the inner ring. Samples were etched using a nital solution. The microstructure was studied in the FEI Nova Nano scanning electron microscope (SEM) and FEI Tecnai Osiris transmission electron microscope (TEM). All SEM images taken are aligned in parallel to the raceway surface. A FEI Helios focused-ion-beam (FIB) system was used to cut out specimens from specific regions for further transmission electron microscopy studies.

3. Results and discussion

The number of revolutions experienced by the examined samples are listed in table 2; both the introduction of hydrogen and an increase in contact pressure naturally reduce the bearing life. The ingress of hydrogen into the inner ring is particularly damaging since early failure is observed when comparing bearing S1 and H1.

Figure 1 shows the damage in bearing H1, along a single crack that runs through the matrix. Near the crack front, residual cementite particles are seen to be cut by the propagating crack. The regions labelled Pre-WEM (precursor to white-etching matter) represents deformed matter that is not fully developed into white-etching

Table 2: Bearing running conditions and the observed type of failure.

ID	Bearing type	H /ppmw	Contact presure / GPa	Revolutions before failure	Type of failure
S1	ACBB	-	3.3	29.3×10^6	Inner ring failure
H1	DGBB	5	3	1.3×10^6	Inner ring failure
H2	DGBB	5	2.4	29.8×10^6	Test stopped due to vibration

matter (WEM), with similar overall morphology but exhibiting plastic flow lines[c] and circular voids. The voids are assumed to be due to the detachment of not fully dissolved residual cementite. The fact that both the flow lines and voids are tiny features within the pre-WEM, these would result in a darker etching region if the observation is made using optical microscopy.[7] Figure 1c shows that the void within the Pre-WEM is much smaller than the surrounding residual cementite in the matrix, the small size (less than 100 nm in diameter) and its distribution along the deformation bands can be explained by the fact that the cementite is decomposed (into smaller size) via the development of high dislocation density region around the cementite particle under the severe plastic deformation.[15,16,17]

Further behind the crack tip, there is another pre-WEM, smaller in size compared with the previously described pre-WEM, probably relating to a different stress experienced in that local region, as determined by the position and the orientation of the crack. At the far side of the crack tip, a well-developed region of white-etching matter (WEM) is observed, indicating that its formation requires time to develop during cyclic loading. As reported by others,[4,18,19] due to its inertness towards etching reagents, the WEM would appear flat and featureless after etching.

Crack formation is not instantaneous, and its propagation is dependent on the contact pressure and the number of rolling cycles. Coupled with the hypothesis[20,21,8,22,23,13,24] that WEM would form on the crack surface region that endures

[c] Also described by West[14] as smeared band structures.

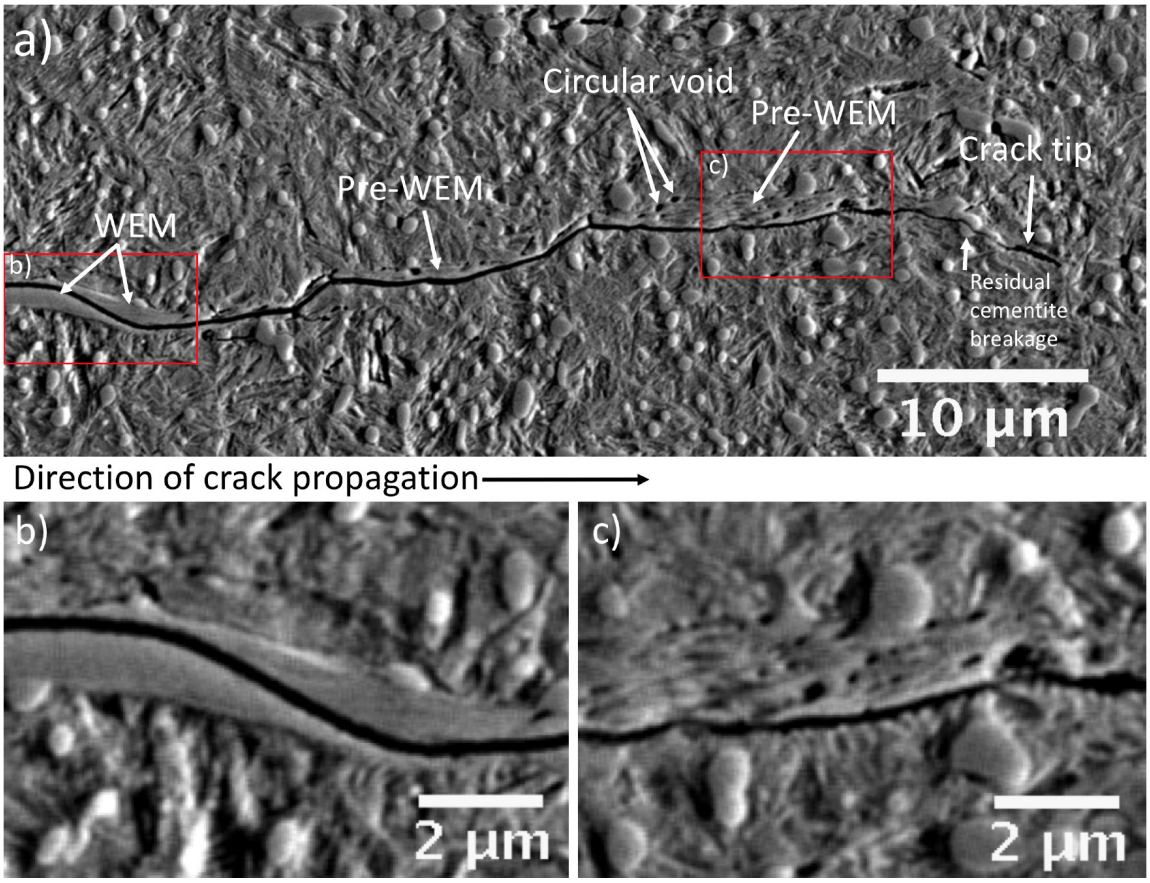

Figure 1: Sample H1, Crack region at 214 µm from contact surface. a) Microstructure evolution observed along a crack with observe associated microstructure features, showing residual cementite breakages by crack propagation and the formation of Pre-WEM and WEM on the crack surface. b) WEM with no observable feature within. c) Pre-WEM with plastic flow lines and voids.

severe surface rubbing, this micrograph confirms the WEM is formed after crack formation. Here, various stages in the evolution of the white-etching matter formation are shown, the severe plastic deformation flow lines within the pre-WEM are observed to be aligned in near parallel direction to the crack surface. The process of structural evolution indicated for WEM is justified by the fact that (1) the crack is not uniformly decorated with white-etching matter, (2) the size of WEM varies with distance from the crack tip and rolling contact surface, and (3) it occurs only on the crack faces that are normal to the compression axis of contact stress.

WEM formation is essentially comparable to other severe plastic deformation processes,[25,26] which begin with the deformation or rubbing of the crack surfaces, where the local region is plastically deformed, and a high dislocation density is developed. An elongated structure is formed on the deformed region and which aligns along the deformation direction (which is nearly parallel to the crack surface in this instance). Any residual cementite would be sheared and can dissolve under such an intense strain. Further rolling contact fatigue cycles would lead to a gradual increase in the misorientations of dislocation cell boundaries which than become the grain boundaries of nano ferrite grains. The carbon introduced by the dissolution of cementite segregate to these cell boundaries.[25]

Figure 2 shows the structure around a branching crack. Other than WEM related features, slip bands are also seen. Multiple crack branching would alter the stress distribution in the surrounding regions, with a more profound stress acting near the WEM region. It is believed that the slip bands are induced there during cyclic loading.

The Hertzian stress at the depth at which the maximum shear stress is encountered, where cracks probably initiate, is more complex with τ, σ_r, σ_θ and σ_z[d] all having finite values. However, away from the depth of maximum shear stress, σ_r and σ_θ become zero, so the deformation mode must be simplified. This might explain the orientation of well-defined slip bands in the region away from the cracks. Table 3 summaries the observed microstructural damage and the resolved shear stress expected in the local region in the vicinity of the crack under a bearing load.

Deformed/sheared residual cementite was also observed within the pre-WEM in figure 2, here the residual cementite remains within the pre-WEM in contrast to the pre-WEM found in figure 1. West and Janakiraman[14,27] made similar observations with respect to cementite (whole and sheared) within the WEM.

Figure 3 reveals a different WEM morphology obtained in bearing H2. Here, multiple cracks were observed. There is a major crack that is related to the observed WEM in the centre of the picture. It is most likely that this WEM was formed to-

[d] τ is shear stress, σ_r, σ_θ and σ_z are stress distribution down the axis r, θ and z.

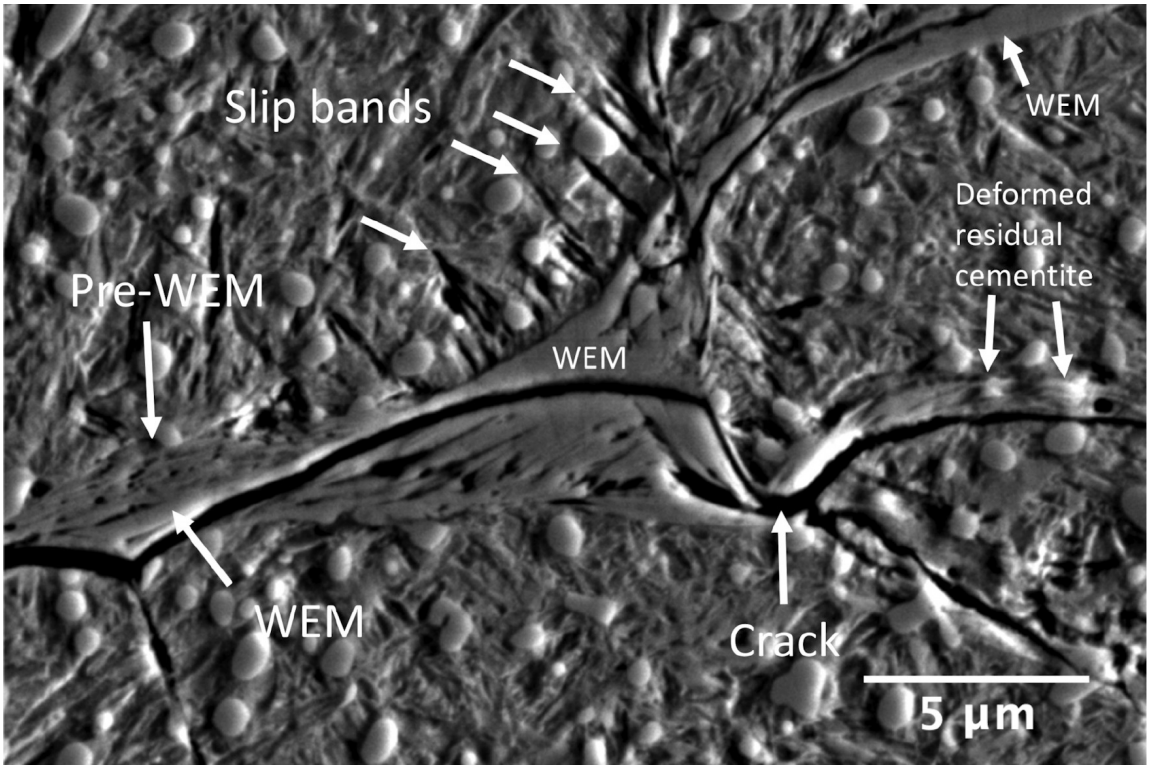

Figure 2: Sample H1, Cracks region at 184 µm from contact surface. a) The microstructure features around a branching crack. Slip bands and deformed residual cementite is observed in addition to pre-WEM and WEM.

gether with the micro crack as indicates on the micrograph. Below the major crack, severe deformation flow lines and residual cementite are observed. The microstructure in this deformed region is akin to Pre-WEM, indicating that the microstructure alteration is less advanced compared to the observed WEM on the other side of the crack.

A new microstructural feature is observed in figure 3, consisting of multiple parallel bands that run across the WEM and Pre-WEM. These are designated 'engineering bands' because (as shown later) they grow after the formation of WEM or Pre-WEM during cyclic loading. Figures 4a and b show SEM images with the engineering bands, with a corresponding higher resolution bright field TEM image in figure 4c and d. Diffraction pattern obtained from indicated region in figure 4d is shown in figure

Table 3: The estimated level of resolved shear stress expected in the vicinity of the crack under a bearing load and the resultant microstructure alteration at the start of WEM formation. Based on the observed microstructural damage.

Region	Stress level	Microstructure alteration
Without crack	As calculated by Hertzian Contact Stress formulation, location dependent, lower than critical resolved shear stress	-
Crack vicinity (2-10 μm away from crack surface)	Higher than the resolved shear stress calculated by Hertzian Contact Stress formulation, lower than the critical resolved shear stress. Also affected by how close in proximity other cracks form.	Slip bands
Crack surface (0-2 μm from crack surface) in the preferable orientation	Significantly higher than the critical resolved shear stress, localised plastic deformation with every bearing revolution.	Pre-WEM and WEM

4e. Surprisingly, the engineering bands are indeed ferrite polycrystals. In agreement with other investigators, the WEM consists of ultrafine ferrite grains.[4,28,29] Here, no residual carbides were observed.

Figure 5 shows an image and the corresponding chromium distribution near the WEM region; the dissolution of cementite distributes the chromium that was enriched in the cementite, homogeneously within the WEM.

The observation and hypotheses of the formation of engineering bands are listed below. The observed features of engineering bands include:

1. Consists of poly-crystalline ferrite that is plate-like in overall shape.
2. Growth across many ultra-fine grains within the WEM in different orientations.
3. The bands are confined to WEM and pre-WEM.

The hypothesis for engineering band formation is:

1. Early crack initiation and crack branching in the hydrogen charged sample that promotes early WEM formation, and enables WEM to experience a large number of stress cycles.
2. The possibility of sub-micrometre adiabatic shearing during rolling contact fatigue. Adiabatic shearing that causes a local temperature increase during

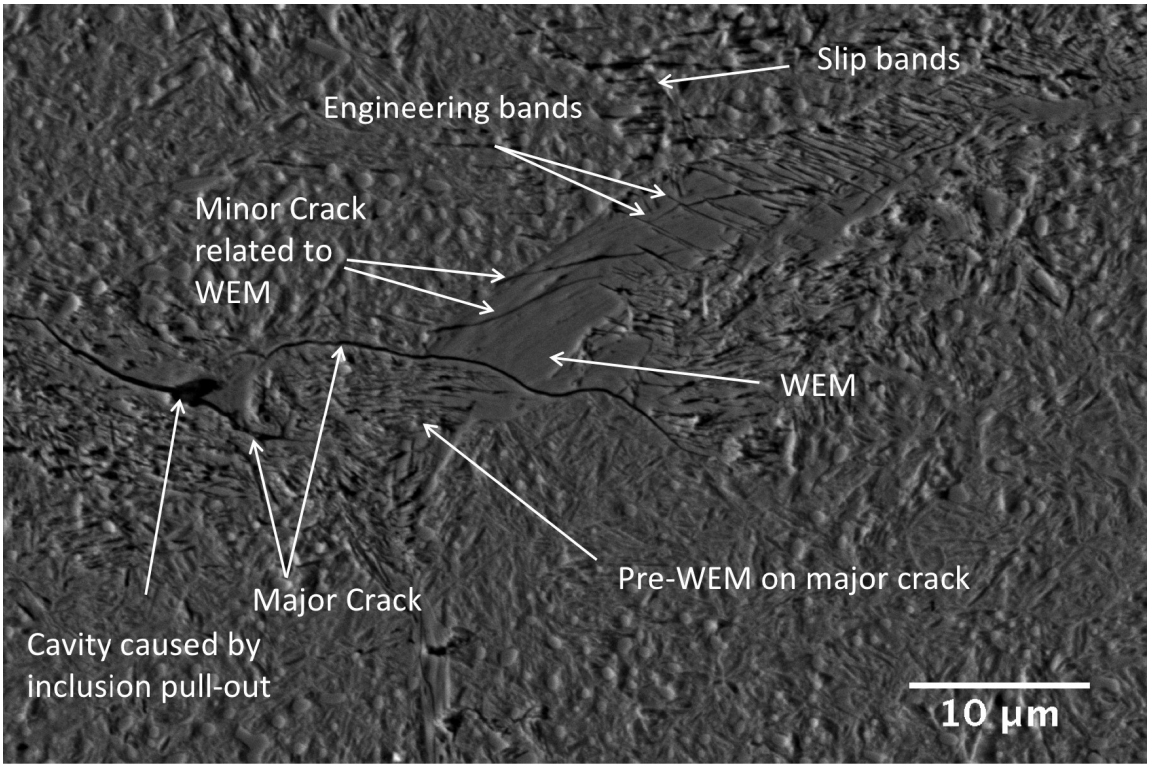

Figure 3: a) Complex microstructure feature observed on sample H2, cracks region at 50-340 µm below surface.

rolling contact would soften the WEM, and hence assists the ferrite plate to grow through WEM.

3. It is confined to WEM or Pre-WEM because a fine-grained or heavily deformed structure would soften more rapidly with increased temperature. It is likely that there are adiabatic shear bands within the WEM.
4. Its formation is time or number of revolutions dependent.

Figure 6a shows sample H2 in as-polished condition. Only cracks and slip bands were observed in the as-polished condition. It is revealed in figure 6b and c that the slip bands did not disappear after re-polishing[e]. The orientation of the persistence

[e]The re-polishing procedure included 6 µm and 1 µm diameter diamond suspension and finishing off with 0.04 µm diameter colloidal silica suspension.

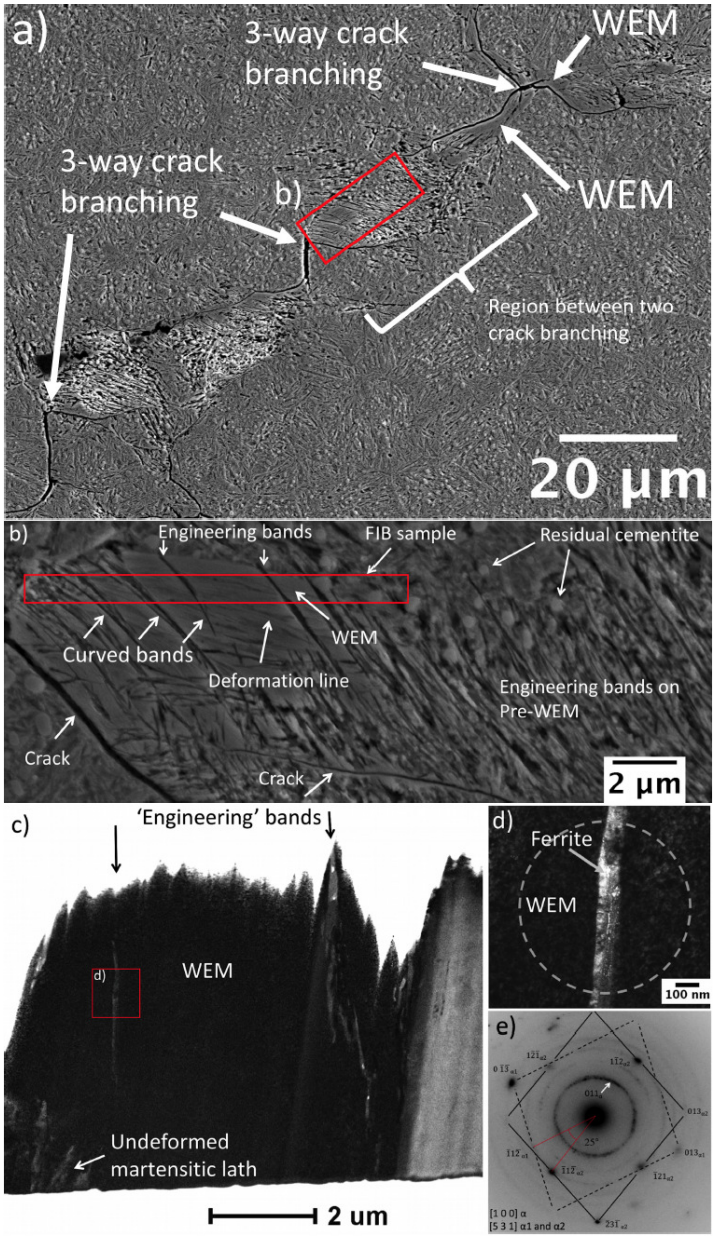

Figure 4: Sample H2, Cracked region at 242 µm below rolling contact surface. a) Three 3-way cracks branching. b) Engineering bands observed within WEM and Pre-WEM. Red rectangular indicates the region of FIB sample is taken. c) Bright field TEM image of FIB sample showing engineering bands within WEM and undeformed martensitic laths without sharp interphase are also observed. d) and e) Magnified single engineering band and its indexed diffraction pattern showing the engineering band are ferrite crystal which are about 100 nm thick. A diffraction pattern of concentric rings indicates the formation of isotropic polycrystal nano size ferrite grains where the spot ring of 011 is indicated.

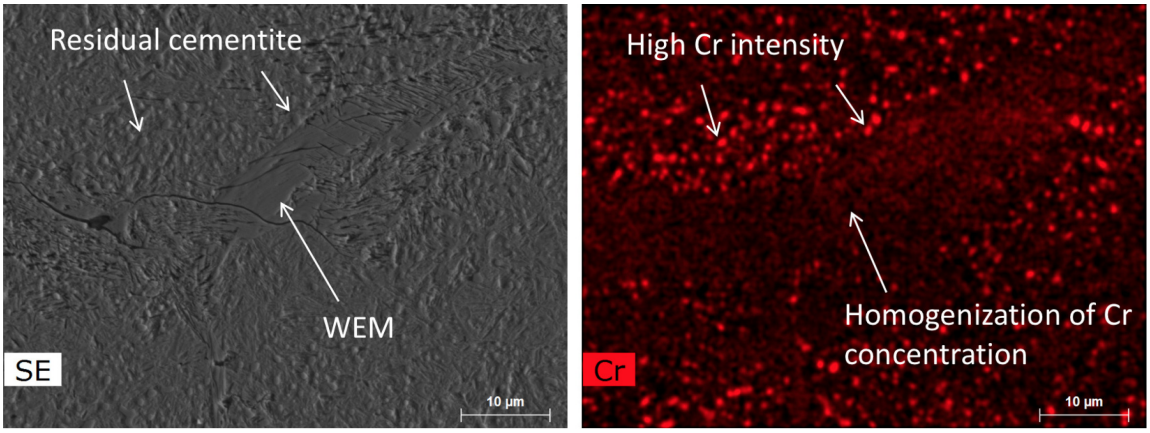

Figure 5: SEM image and the corresponding chromium intensity map. Homogenization of chromium element is observed with the WEM region.Cracks region 50-340 µm below rolling contact surface.

slip bands remains the same. A noticeable difference between figure 6a and b is that one of the slip traces has become more broadened with wider lines with rather hazily defined edges. Other slip traces, however, seem to become thinner. The observed characteristic of the slip bands is similar to the one described in rotating bending samples as describe by Ewing[31] back in 1903. It has been shown in figure 2 and 3 that slip bands are present in both sample H1 and H2. It has been demonstrated here that the slip bands are formed in the matrix and are typically surrounded by multiple cracks but the slip bands are away from the crack surfaces. As there is no evidence that the cracks observed are initiated from the slip bands, it can be concluded that the slip bands observed in this study are formed after the crack formation, resulting from the change in stress distribution experienced in this local area and localised cyclic fatigue[f].

Figure 7 compares the traced cracks observed on both hydrogen charged samples tested at different contact pressure a) 2.4 GPa (H2) and b) 3 GPa (H1)[g]. The crack

[f]This simple re-polishing procedure would provide a microscopic evident to support any claims that the cracks could be initiated from the slip bands in WEC.

[g]The aim of this exercise is not to compare the severity of crack networks in two bearings which may require more than one micrograph from each condition, but to compare the cracking behaviour and morphology, which the author believe one micrograph from each condition is representative.

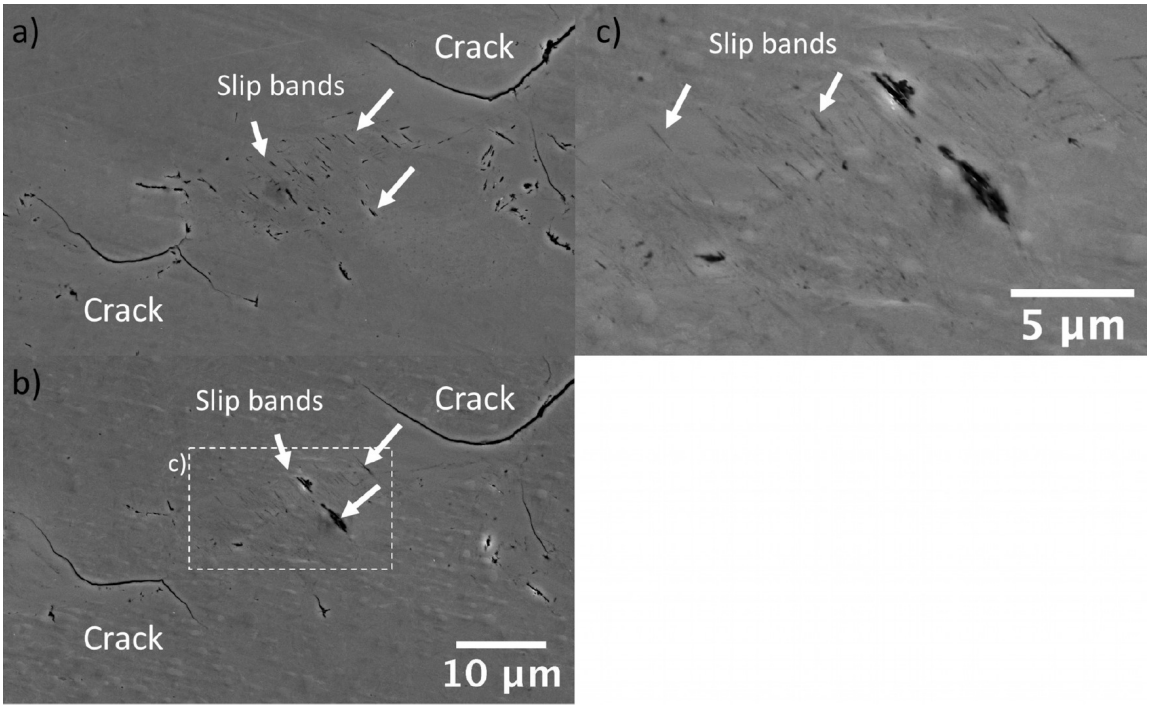

Figure 6: Sample H2, region between 180-220 µm from rolling contact surface. a) As polished micrograph showing slip bands between two cracks. b) The re-polished surface in the same area as a) showing the same slip bands region. c) High magnification of slip bands with indication of slip bands are cavities.

morphology observed in figure 7a are difference from those of figure 7b. The crack networks observed in sample H2 are numerous and dense compared to one found in H1. Furthermore, the multiple cracks seen in the H2 sample are not linked (figure 7a), and at high magnification, multiple micro-cracks(figure 7c) were also observed, indicating that the branching of crack behaviour on both samples are different.

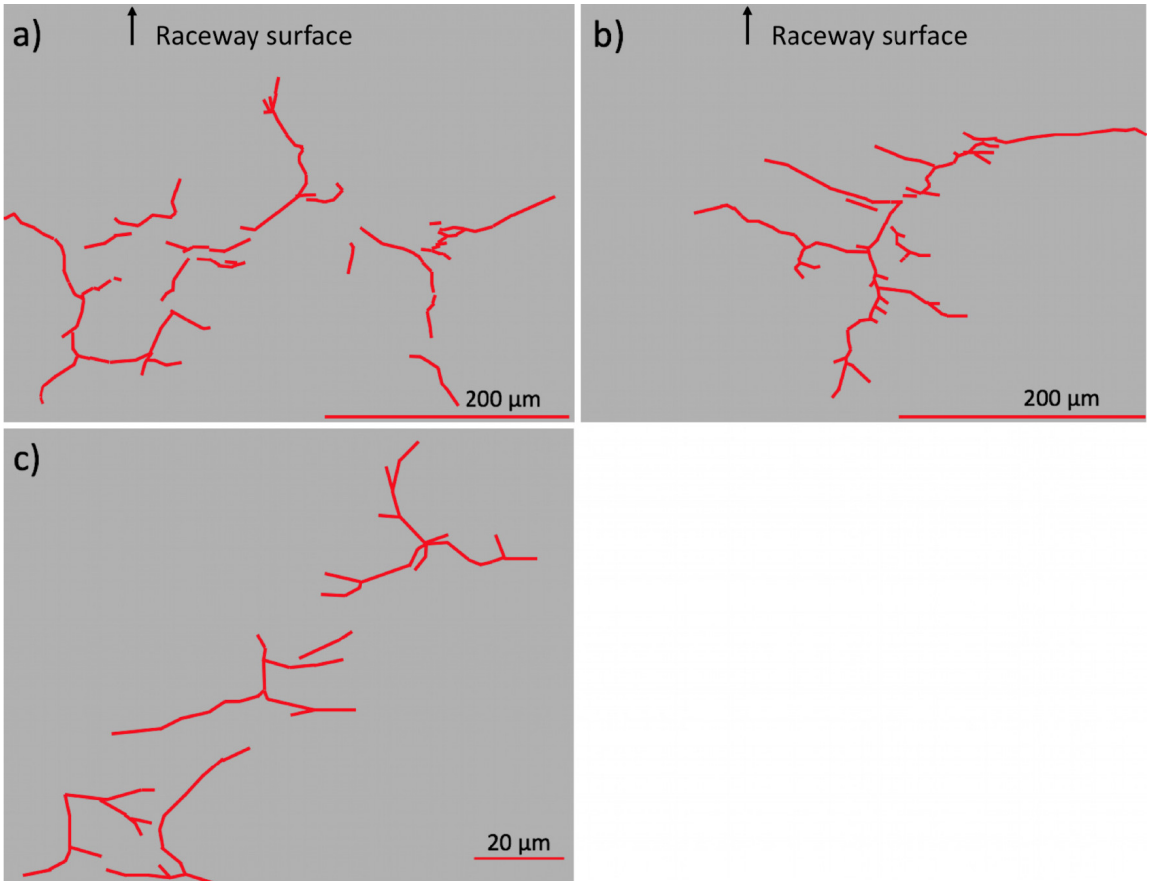

Figure 7: Trace cracks observed in bearing H1 and H2. Both inner rings have been hydrogen charged but tested at different contact pressure a) 2.4 GPa (H2) b)3 GPa (H1) c) Same as figure a, but at high magnification. The rolling contact surface on the bearing is indicated on both figures a and b. The centre position of figure c is 150 µm below the rolling contact surface.

In order to compare the hydrogen-charged bearings with a standard bearing, one non-hydrogen-charged bearing was investigated. Figure 8 compares the altered microstructure obtained near the surface spall in bearing S1 and H2. In the bearing

that has been hydrogen charged and tested at low contact stress of 2.4 GPa, the observed damage includes a larger WEM with engineering bands and slip bands. The existence of these microstructural features indicates that a high number of stress cycles have been experienced in the region of cracks. Without hydrogen charging but tested at a higher contact stress, the observed damage near the surface spall is a small WEM with no observable engineering bands, nor any sub-surface WEC in the failed bearing.

With a similar number of revolutions experienced by both bearings S1 and H2 before failure, it is possible to explain the combined effect of hydrogen and contact stress on early bearing failure. Previous work[32,18,33,34] has identified material defects, particularly the non-metallic inclusions as the WEC initiators. It was also shown in this work that the introduction of hydrogen into the bearing would induce early cracking.

The bearing subsurface microstructure damage starts with an early crack formation that changes the stress distribution in their vicinity that then leads to the microstructure alteration with the WEM, engineering bands within WEM and slip bands formation during the continuation of bearing testing. The increase in contact pressure in the presence of hydrogen would promote the development of the crack systems which grow into considerable sizes that eventually trigger spalling that causes bearing failure after a short testing time; in this bearing testing condition, only slip bands, pre-WEM, and WEM formation are observed. Without hydrogen ingress but tested at high contact stress, the crack initiation from the stress concentrator (most likely to be non-metallic inclusion) will take a long time, however, once the crack is initiated, the crack propagation can be rapid and will cause the bearing to spall and fail. Since the crack propagation is fast, there is limited time for other cracks to develop in parallel and there by limited or no observable WEC will be formed.

Based on the detailed microstructure analysis in this work, it is proposed that the microstructure damage of white-etching crack begins with crack initiation. The crack initiation and branching that develops into a microscopic network should alter the local stress distribution which leads to the different level of local deformation. The intense plastic deformation begins with the formation of Pre-WEM followed by

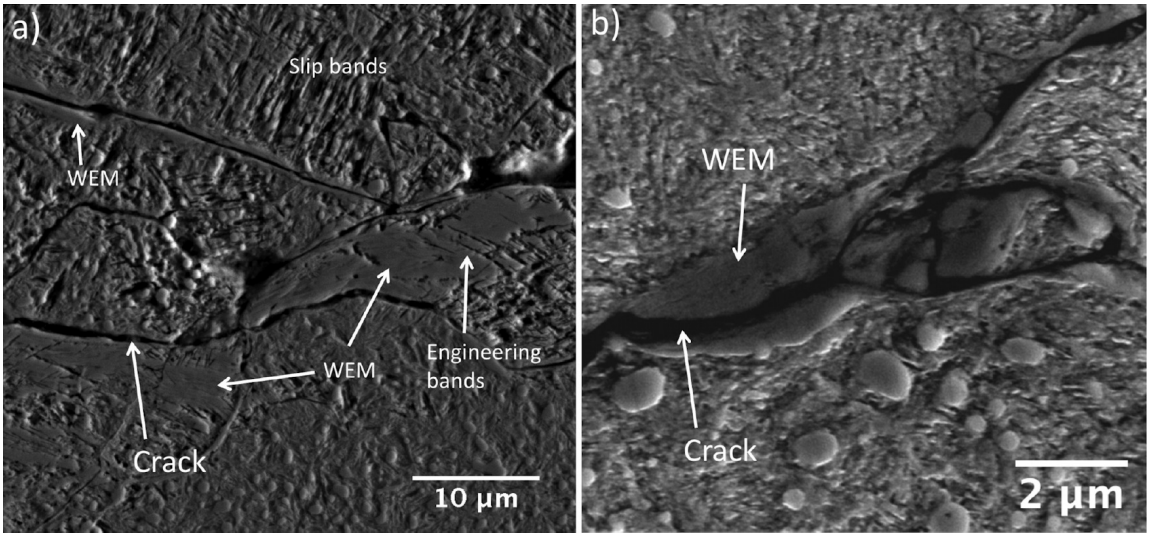

Figure 8: a) Large WEM with engineering bands and slip bands observed near the surface spall in hydrogen charged bearing, H2. b) Small WEM without engineering band and no slip bands observed on the non hydrogen charge bearing, S1.

WEM on the crack surface during the continuation of cyclic loading[h]. The initiation of crack and crack branching that changes the local stress distribution allow the planar slip bands to form in the crack vicinity. Depending on the applied contact pressure, the continuation of the bearing operation will lead to the formation of engineering bands within the Pre-WEM and WEM. The major difference between the slip bands and engineering bands is that slip bands are formed on the matrix, while engineering bands form on Pre-WEM and WEM. Furthermore, slip bands can be observed on the as-polished surface.

Conclusions

A detailed microstructure investigation on white-etching crack containing failed ball bearing inner rings reveals that

1. The sequence of the microstructure alteration observed in WEC containing bearing steel is as follows: On the crack surface, the pre-WEM is formed first

[h]The crack would continue to propagate and to branch under the cyclic loading.

and followed by WEM and engineering bands. At the crack vicinity, the slip bands are formed.

2. The microstructure evidence obtained in this work supports the idea that all observable microstructure alterations are formed after the crack formation.
3. Subsurface cracks are promoted by hydrogen ingress. However, under low contact pressure, bearing failure is slowly initiated. The continuation of bearing testing in the presence of microcracks aids the microstructure damage with the formation of WEM, slip bands and engineering bands.
4. In the presence of hydrogen and high contact pressure, the crack propagation is rapid which results in early bearing failure. The subsurface microstructure damage observed is large crack networks associated with slip bands, Pre-WEM and WEM.

Acknowledgements

The authors are grateful to SKF for the provision of samples and financial support, and to Professor Sir Harry Bhadeshia and Steve Lane for helpful discussion and comments.

Reference

[1] K. Tamada and H. Tanaka: 'Occurrence of brittle flaking on bearings used for automotive electrical instruments and auxiliary devices', *Wear*, 1996, **199**, 245–252.

[2] K. Tamada, H. Tanaka, and N. Tsushima: 'A new type of flaking failure in bearings for electrical instruments of automotive engines'in 'Bearing Steels: Into the 21st Century', (ed. J. J. C. Hoo and W. B. Green) **1327**, 167–185, 199, USA, American Society for Testing and Materials.

[3] K. Iso, A. Yokouchi, and H. Takemura. 'Research work for clarifying the mechanism of white structure flaking and extending the life of bearings', *SAE Technical Papers*, 2005, 2005-01-1868, DOI:10.4271/2005-01-1868.

[4] M.-H. Evans. 'An updated review: white etching cracks (WECs) and axial cracks in wind turbine gearbox bearings', *Materials Science and Technology*, 2016, **32**, 1133-1169.

[5] M.-H. Evans. 'White structure flaking (WSF) in wind turbine gearbox bearings: Effects of 'butterflies′ and white etching cracks (WECs)', *Materials Science and Technology*, 2012, **28**, 3–22.

[6] H. Uyama and H. Yamada. 'White structure flaking in rolling bearings for wind turbine gearboxes', *Wind Systems*, May 2014, 14–25.

[7] K. Stadler, J. Lai, and R.H. Vegter. 'A review: The dilemma with premature white etching crack (WEC) bearing failures', In *Bearing Steel Technologies: 10th Volume, Advances in Steel Technologies for Rolling Bearings*, 2015, STP 1580, 487–508.

[8] H.K.D.H. Bhadeshia and W. Solano-Alvarez. 'Critical assessment 13: Elimination of white etching matter in bearing steels', *Materials Science and Technology*, 2015, **31**:1011–1015.

[9] H. Uyama, H. Yamada, H. Hidaka, and N. Mitamura. 'The effects of hydrogen on microstructural change and surface originated flaking in rolling contact fatigue', *Tribology Online*, 2011, **6**, 123–132.

[10] B. Han, B.X. Zhou, and R. Pasaribu. 'C-ring hydrogen induced stress corrosion cracking (HISCC) tests in lubricating liquid media', In *European Corrosion Congress*, 2011, **1**, 615–623.

[11] M. N. Kotzalas and G. L. Doll. 'Tribological advancements for reliable wind turbine performance', *Philosophical Transactions of the Royal Society A*, 2010, **368**, 4829–4850.

[12] J. A. Ciruna and H. J. Szieleit 'The effect of hydrogen on the rolling contact fatigue life of AISI 52100 and 440C steel balls', *Wear*, 1973, **24**, 107–118.

[13] R. H. Vegter and J. T. Slycke. 'The role of hydrogen on rolling contact fatigue response of rolling element bearings', *Journal of ASTM International*, 2010, **7**, ID JAI 102543.

[14] O.H.E. West, A.M. Diederichs, H. Alimadadi, K.V. Dahl, and M.A.J. Somers. 'Application of complementary techniques for advanced characterization of white etching cracks', *Praktische Metallographie/Practical Metallography*, 2013, **50**, 410–431.

[15] Y. Ivanisenko, W. Lojkowski, R. Z. Valiev and H. J. Fecht. 'The mechanism of formation of nanostructure and dissolution of cementite in a pearlitic steel during high pressure torsion', *Acta Materialia*, 2003, **51**, 5555–5570.

[16] M. H. Hong, W. T. Reynolds Jr., T. Tarui and K. Hono. 'Atom Probe and Transmission Electron Microscopy Investigations of Heavily Drawn Pearlitic Steel Wire', *Metallurgical and Materials Transactions A*, 1999, **30**, 717–727.

[17] S. Ohsaki, K. Hono, H. Hidaka, and S. Takaki, 'Characterization of nanocrystalline ferrite produced by mechanical milling of pearlitic steel', *Scripta Materialia*, 2005, **52**, 271–276.

[18] M.-H. Evans, A.D. Richardson, L. Wang, and R.J.K. Wood. 'Serial sectioning investigation of butterfly and white etching crack (WEC) formation in wind turbine gearbox bearings', *Wear*, 2013, **302**, 1573–1582.

[19] R. Errichello, R. Budny, and R. Eckert. 'Investigations of bearing failures associated with white etching areas (WEAs) in wind turbine gearboxes', *Tribology Transactions*, 2013, **56**,1069–1076.

[20] K. Hiraoka, M. Nagao, and T. Isomoto. 'Study of flaking process in bearings by white etching area generation', *Journal of ASTM International*, 2007, **3**, 234–240.

[21] P.M. Anderson, N.A. Fleck, and K.L. Johnson. 'Localization of plastic deformation in shear due to microcracks', *Journal of the Mechanics and Physics of Solids*, 1990, **38**, 681–699.

[22] W. Solano-Alvarez and H.K.D.H. Bhadeshia. 'White-etching matter in bearing steel. Part I: Controlled cracking of 52100 steel', *Metallurgical and Materials Transactions A*, 2014, **45**, 4907–4915.

[23] W. Solano-Alvarez and H.K.D.H. Bhadeshia. 'White-etching matter in bearing steel. Part II: Distinguishing cause and effect in bearing steel failure', *Metallurgical and Materials Transactions A*, 2014, **45**:4916–4931.

[24] A. Grabulov, R. Petrov and H.W. Zandbergen. 'EBSD investigation of the crack initiation and TEM/FIB analyses of the microstructural changes around the cracks formed under rolling contact fatigue (RCF)', *International Journal of Fatigue*, 2010, **32**, 576–583.

[25] J.-H. Kang, B. Hosseinkhani, C.A. Williams, M.P. Moody, P.A.J. Bagot, and P.E.J. Rivera-Díaz del Castillo. 'Solute redistribution in the nanocrystalline structure formed in bearing steels', *Scripta Materialia*, 2013, **69**, 630 – 633.

[26] K. Hiraoeca. 'White-type microstructural change in rolling contact fatigue from the viewpoint of severe plastic deformation', *Tetsu-To-Hagane/Journal of the Iron and Steel Institute of Japan*, 2008, **94**, 636–643.

[27] S. Janakiraman, P. Klit, N.S. Jensen, and J. Gronbaek. 'Observations on the effects of grooved surfaces on the interfacial torque in highly loaded rolling and sliding tests', *Tribology International*, 2015, **81**, 179–189,.

[28] A. Grabulov, U. Ziese, and H.W. Zandbergen. 'TEM/SEM investigation of microstructural changes within the white etching area under rolling contact fatigue and 3-D crack reconstruction by focused ion beam', *Scripta Materialia*, 2007, **57**, 635–638.

[29] P. C. Becker. 'Microstructural changes around non–metallic inclusions caused by rolling–contact fatigue of ball–bearing steels', *Metals Technology*, 1981, **8**, 234–243.

[30] H. K. D. H. Bhadeshia. 'Modelling of recrystallisation in mechanically alloyed materials', *Materials Science and Engineering A*, 1997, **A223**, 91–98.

[31] J. A. Ewing and J. C. W. Humfrey. 'The fracture of metals under repeated alternations of stress', *Philosophical Transactions of the Royal Society of London A: Mathematical, Physical and Engineering Sciences*, 1903, **200** (321-330), 241–250.

[32] M.-H. Evans, A.D. Richardson, L. Wang, R.J.K. Wood, and W.B. Anderson. 'Confirming subsurface initiation at non-metallic inclusions as one mechanism for white etching crack (WEC) formation', *Tribology International*, 2014, **75**, 87–97.

[33] T. B. Lund. 'Sub-surface initiated rolling contact fatigue—influence of non-metallic inclusions, processing history, and operating conditions', *Journal of ASTM International*, 2010, **7**, JAI102559.

[34] A. R. Du Crehu. 'Tribological analysis of White Etching Crack (WEC) failures in Rolling Element Bearings', PhD thesis, L'Institut National des Sciences Appliquées de Lyon, France 2014.

4. Appendix

Table 4 lists the definition and description of the microstructure used in this work.

Table 4: The microstructure description and definition use in this work

Microstructure	Definition and description
Matrix	Main microstructure of the steel-typically tempered martensite
Residual cementite	Pro-eutectoid cementite precipitate that did not dissolve during austenitzation, spherical particle that has different contrast to the matrix after etching
Crack	An irregular line/plane that appear to split two surfaces without breaking apart, the tip of the crack can be pointy.
Circular void	A cavity that is due to the particle drop off, appear dark and circular
White-etching matter (WEM)	Contains ultra-fine ferrite with carbon atom distributed on the grain(cell) boundaries, region that appears white when examined under optical microscope, featureless and flat region when examined under SEM. In this work, we are not using the term white-etching area(WEA) and white-etching constituent(WEC) since this microstructure is in three dimensional and the abbreviation of white-etching constituent may be confuse with the abbreviation white-etching crack.
White-Etching Cracks (WEC)	A three-dimensional branching crack networks that appear on the subsurface of failed bearing may link to the surface, with WEM appear adjacent to the cracks.
Precursor to white-etching matter (Pre-WEM)	Has the same morphology and shape of white-etching matter with deformation flow line, sheared residual cementite and circular void can be seen within the structure
Engineering bands	Consist of ferrite crystal that appear within WEM and Pre-WEM after long rolling contact cycle
Slip bands	Each slip trace is a thin line that appears in an unetched condition. Typical appear in more than one straight line in parallel on the matrix.